Transient behaviors of centrifugal pump operation under air-entraining vortices

Ali Hassan Hammoud
Department of Mechanical Engineering, Beirut Arab University, Beirut, Lebanon

An experimental study was undertaken to provide means by which the air entraining vortices affect the centrifugal pump performance. The measurements taken included; the pump pressure head, discharge, input power and sound pressure level, which were recorded along a test of 120 seconds. The results indicated that the pump performance was badly affected in transient way. It was also demonstrated that, the automatic control variation of the pump speed under air entraining region could be harmful to pump and can shorten its lifetime.

أجريت دراسة معملية لتعيين تأثير العمق الغاطس الحرج و الدوامات الساحبة للهواء و سرعة تشغيل المضخة علي أداء مضخة طاردة مركزية. وقد أخذت قياسات معملية تشتمل علي قياس ضاغط المضخة، التصرف، القدرة المستهلكة و شدة الضوضاء المنبعثة. وقد سجلت هذه القياسات خلال فترة زمنية قدرها ١٢٠ ثانية. بالإضافة إلى هذه القياسات تم تصوير و تسجيل الدوامات الساحبة للهواء في منطقة مدخل المضخة كما تم أيضا دراسة أثر استخدام التحكم الاتوماتي في سرعة المضخة باستخدام مغير التردد.

وقد أوضحت نتائج هذه الدراسة أن أداء المضخة يتأثر تأثيرا خطيرا أثناء تولد الدوامات الساحبة للهواء عند مدخل المضخة. كما أن التحكم الاتوماتي لتغير سرعة المضخة أثناء وجود هذه الدوامات له تأثير مدمر علي المضخة.

Keywords: Centrifugal pump, Vortex, Transients, Air-entraining.

1. Introduction

Nowadays, the increases in water demand and storage for drinking, domestic, agriculture, hydraulic power stations, and for cooling electrical power generating plants (by circulating a large amount of water from pools or reservoirs etc..) need optimum installation of pumps. The proper installation means high efficiency of operation, low cost per unit of discharge, self-priming and less troubles. By giving proper attention to the design and construction of sumps as well as correct selection and installation of the pumps, vibration and cavitation may be eliminated. This means less damage, of impeller and bearing and consequently less maintenance cost and longer pump life.

When an intake has to be located in relatively shallow water because of construction cost considerations or because no deep water is available, critical submergence can provide considerable advantages. The determination of the critical submergence of an intake of a pump sump is usually a critical decision since it defines the lowest point of pumping station. In general, the submergence of an intake should be large enough to reduce the possible occurrence of air entraining vortices. The value of submergence of the intake when air-entraining vortex just tends to enter the intake is called " critical submergence".

Pump intake vortices and the methods for their suppression have generated much interest during the past several decades. The usual solution is to conduct laboratory experiments on scaled models to identify the source of particular problems and find solutions to eliminate them. For example, Denny [1] reported an experimental study of the factors affecting air -entraining vortices in pump sumps using several models of different sumps.

He concluded that regular and repeatable vortices were generated when the swirl existed in the sump or when the pipe was located at the swirl center. Furthermore, a significant drop in efficiency was also observed when air from vortices entered the suction inlet of the pump. Denny and Young [2] continued Denny's study to prevent the vortex formation by using baffle walls or floating rafts. They found that, in extreme cases, over 10% of the flow entering the intake could consist of air, and swirling angles of up to 40% could be realized thereby resulting in disastrous effects

on the pump.

Many other researchers studied the critical submergence related to intake in still-water tanks reservoir. Several studies presented by Anwar [3, 4] and Odgaard [5] indicated that the critical submergence is depending on Froude number and circulation.

Jain et al. [6] found that the liquid viscosity decreases the critical submergence ratio while the surface tension has no effect.

Recently, Elshorbagy and Warda [7] constructed a sump made of Plexiglas tank in order to investigate the cavitation noise at the inverted intake. As a first step in their investigation, they tested the variation of critical submergence with the mass flow rate using two different pipes size 1.9 and 2.5-cm. They found that, the critical submergence ratio increases as the intake velocity increases while for a given intake velocity, the critical submergence ratio is slightly smaller for larger intakes than for smaller intakes. They also concluded that cavitation noise emitted from inverted pipe intakes could be used as a log for the recognition of the onset of cavitation as well as its subsequent stages.

Warda [8] reported another experimental study to investigate the flow characteristics in the gap between the buffer plate of a vortex breaker and the bottom of a floating roof tank. He measured the pressure profile for a gap thickness of 2 and 5 mm at various submergence. He found that the pressure decreased rapidly towards the intakes due to the increasing radial velocity and when the flow reached the edge of the intake pipe, the pressure started to rise again. Furthermore, he found that the vortex formation is strongly dependent on the vortex breaker height over the tank bottom. Additionally, he recommended that the vortex breaker should be installed closer to the draw off nozzle in order to avoid the formation of weak vortices. He concluded that the height of the vortex breaker over the tank bottom has a significant effect on the swirl and vortex formation at the intake. Also the flow rate affects the extent of pressure depression in the core, and strength of vortex. Yildirim et al. [9] studied the critical submergence for air-entraining vortex at intakes in a uniform channel- flow with pipe diameters varying from 30 to 100 mm. They concluded that, more critical submergence ratio could be obtained at lower clearance and more flange diameter. In their following paper [10], they presented a formula for critical submergence of intakes in still water tank, which relates the intake discharge, diameter, velocity and the critical velocity to the critical submergence. They concluded that, the critical velocity depends on flow geometry and varies with clearance of the intakes.

From the previous literature review, it is clear that the air entraining vortices at the pump intake was treated as steady flow problem. To the knowledge of the author, no research work till now treats this problem as a transient problem, i.e. they always neglect the time parameter effect.

The aim of this paper, is to study the effect of critical submergence, air entraining vortices and pump rotational speed on the pump performance includes pressure head, discharge, power and efficiency. Results are presented as a time function.

Additionally, the automatic application of variable speed pump driven by a frequency inverter in the region where air-entraining vortices occurred was also analyzed.

2. Experimental set up and instrumentation

Test rig was designed and tested for this particular study. As shown in fig 1, water from steel tank 2×2×1.2 m was re-circulated by means of a centrifugal pump driven by a 3 phases 6 kW motor operated on frequency inverter variable speed drive type (Hitachi L100). Two fine mesh screens were used to ensure as wave free uniform flow possible. The suction pipe of 0.152 m diameter was made of Perspex for visual investigation of the flow at the inlet and inside the pipe.

The intake configuration presented in this study is more preferable than other shapes in muddy water supply and rivers. This shape ensures water intake from the upper layer with less sediment concentration (i.e. less harmful effects to the pumping system).

The centrifugal pump used in this investigation has a radial flow type impeller. This pump has the following specifications at the best efficiency point: 63 % efficiency,

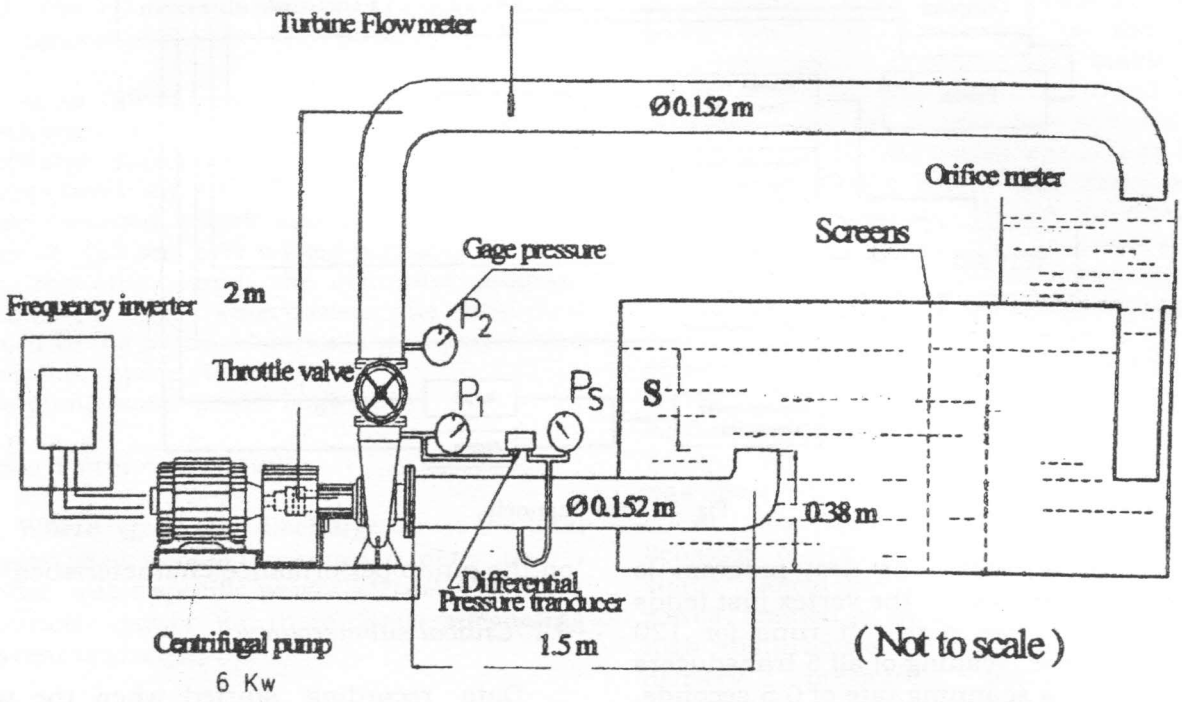

Fig. 1. General layout of the experimental apparatus.

discharge Q = 40 L/s and pump head H= 6 m when running at rotational speed of 1200 R.P.M. with the specific speed of 196 (S.I. units).

A differential pressure transducer is used to measure the suction and delivery pressures, whereas the discharge from the pump is measured by a calibrated orifice meter and turbine flow meter. The pump speed can adjusted manually or automatically depend on test requirement. The vibration of the pump casing was measured using CEL-221 digital vibration meter kit. The measurement of the overall sound pressure level (S.P.L.) is recorded using 1/2 inch Bruel and Kjaer microphone located at a distance of 0.5 m from the axis of the intake. The Bruel and Kjaer microphone provides a direct reading of a range of 24 -130 dB with a reference pressure of 0.00002 N/m^2. Acoustical calibration of the complete instrument is carried out using a Pistonphone Type 4220. The background level was also checked and found to be negligibly contributing to the recorded levels. Data acquisition type (Eurosmart PC-MES3 DATA Acquisition/ Switch Unit) was used for receiving data signals from the several sensors such as: differential Pressure transducer, electrical current (I), vibration meter kit, 1/2 inch Bruel and Kjaer microphone (S.P.L.), turbine flow meter (L/s), and the pump rotational speed (R.P.M.). All these data were recorded every 0.5 second. Fig. 2 shows the arrangement of data channels and their connection to the data acquisition system. All instruments were calibrated in site. The response equation and curve of each instrument was obtained by measuring the corresponding voltage for 10 different readings. The response equations are then introduced in the computer program. However, in order to estimate random error (repeatability), some of the experimental runs were repeated more than one time. Measurements are believed to be accurate to within ±5 % for the S.P.L., ± 3% for the pump pressure head and ± 6% for the discharge. Two HP-BASIC programs were especially

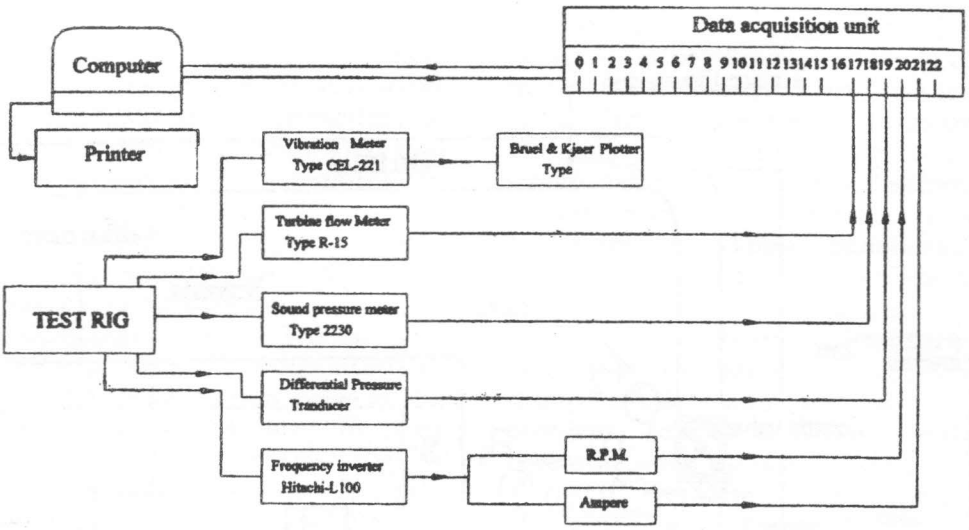

Fig. 2. Data Channels.

written for this study. The first program is started manually when the vortex just tends to enter the intake pipe. It runs for 120 seconds and the reading of all 5 transducers are recorded at a scanning rate of 0.5 seconds. The program plots directly the data of the S.P.L., the pump pressure, vibration level, current (A) and the R.P.M. as a function of time, whereas the overall pump efficiency and pump input power are calculated and then plotted on the screen.

The program has the ability to operate under constant or variable pump speed. The second program is used to record data at a step of 100 R.P.M. It records the variation of the S.P.L. discharge, delivery pressure against the R.P.M.

All tests were carried out under the following conditions: The maximum discharge of the centrifugal pump was around 45 L/s. The ambient temperature in the laboratory was approximately 20°C. The atmospheric pressure is around 101 Kpa.

3. Experiment procedure

Three different procedures were used during this investigation: The first is to determine the critical submergence. The second is to study the pump delivery head against the rotational speed. The third is to examine the effect of air- entraining vortices on the pump performance characteristics.

3.1. Critical submergence

Data recording started when the water level in the tank attains steady state during pump operation. Observation was made over 30 to 60 minutes to determine whether the flow is free from surface vortex or not. If no air vortex core occurred, the water level in the tank was reduced by opening the drain valve. The submergence was decreased by a value of 3 cm each test. During each run when the water level in the tank attains a constant level, the rotational speed was increased gradually and then the measurements were taken. Through all tests, the delivery valve was kept fully open. These steps were repeated each run during which the rotational speed was increased and decreased manually.

3.2. Delivery head

At a particular submergence, the pump was started and the discharge was increased by gradually increasing the rotational speed of the pump through increments of 100 R.P.M from 0 up to 1450 R.P.M. Data signals from the delivery pressure transducer were recorded.

3.3. The effect of air- entraining vortices on the pump performance

At a given submergence and constant discharge, the data signals of the S.P.L., the discharge (L/s), the differential pressure (total pump head m) and the electrical current (I) were recorded simultaneously at a scanning rate of 0.5 sec. over a fixed period of 120 sec. On the other hand, the computer program calculated the waterpower, the absorbed power of the pump (electrical input power) and overall pumping efficiency.
The pump water-power is given by:

$$\text{Water Power} = \gamma.h.Q \ (kW)$$

Where Q is the discharge, h is the total pump head, across the pump in meter, and γ is the water specific weight kN/m^3. The input electrical power for three-phase alternating current is given by:

$$P = 1.732 \ . \ V \ . \ I \ . \ \text{Cos} \ \varphi / 1000 \ (kW),$$

where I is the current, A, V is the voltage at terminals and Cos φ is the power factor.

$$\text{Overall efficiency} = \frac{\text{Water Power}}{\text{Input Power}}$$

$$= \text{Motor efficiency} \times \text{Inverter efficiency} \times \text{Pump efficiency}$$

Knowing the efficiency of motor and inverter from manufacturer catalogue then the pump efficiency can be estimated.

4. Observations

When the water level above the intake was decreased slowly for a constant pump speed and discharge, weak vortices appear at a certain water level. These vortices did affect neither the pump head nor the pump input power. Sometimes, twin weak vortices did appear without any effect. However, with further reduction in water level above the pump intake, long tail vortex appeared and moved towards the center of the intake. Photo.1 shows a vortex just before entering the intake. This noiseless vortex has the shape of a funnel. With further reduction in the water level or increasing in the pump rotational speed, a strong and stable noisy vortex appeared. The "emitted sound" in the area of vortex got louder. Few minutes later, the diameter of the vortex was getting bigger and air-entraining vortex was developed as shown in Photo. 2. When air-entraining vortex occupied the intake, a sudden drop in the pump delivery pressure was observed followed by a drop in the pump-input power and increase in the vibration level.
Photo. 3 shows the noisiest type of a long tail vortex. Small amount of air from the free surface continued to enter the pump intake without affecting on the pump performance was observed.

At low submergence, the shape and behavior of the vortex became different; its shape looked like a horseshoe. The fluctuated waves created by this type of vortex generated high disturbance at the water surface. The delivery pressure fluctuated almost periodically, the discharge tends to break off and the pump was about to turn off.

In order to visualize the air bubbles behavior inside the pump, a small test rig having a transparent pump geometrically similar to the initial one of scale 1:20 was constructed. With the aid of this transparent pump, it was possible to follow and observe clearly the movement of the air stream and air bubbles inside the pump casing. The observation recorded by a video camera demonstrated that when air was entering the pump, it created a stream of minute, fine air bubbles circulating around the impeller of the pump. At this moment, the delivery pressure dropped sharply and then increased again when air bubbles were relieved from the pump. The appearance of air bubbles could be easily detected when the water color became milky (See Photo. 5).

5. Results and discussions

Figure 3 shows the variation of critical submergence S_C with the pump rotational speed. The plot shows two different regions separated by the critical line representing (Sc-Q) curve: No air- vortex region on the left side of curve and air -entraining vortex region on

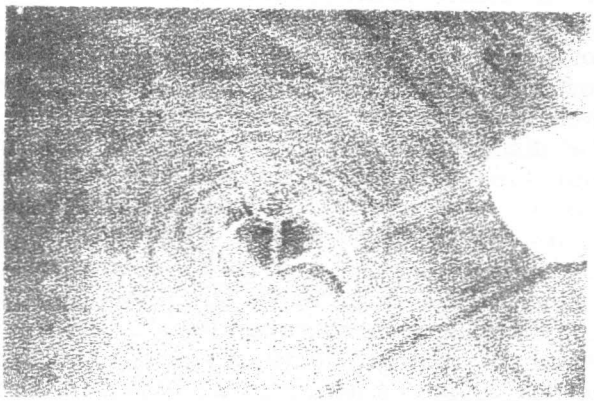

Photo. 1. Vortex just before entraining the intake (type a).

Photo. 2. Developed air-entraining vortex (type b).

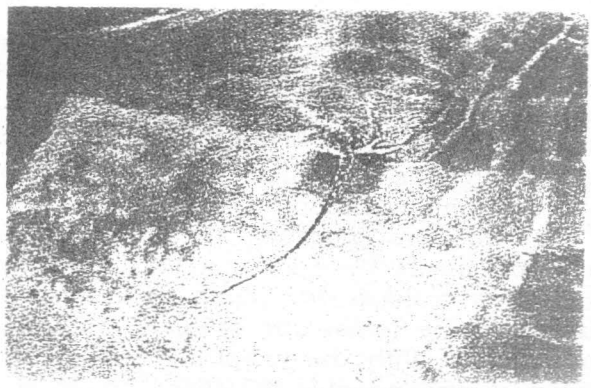

Photo. 3. Noisiest type of long air vortex (type c).

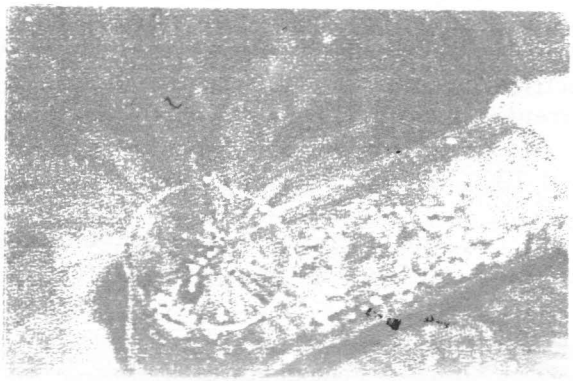

Photo. 4. Vortex as sorbing large quantity of air (type d).

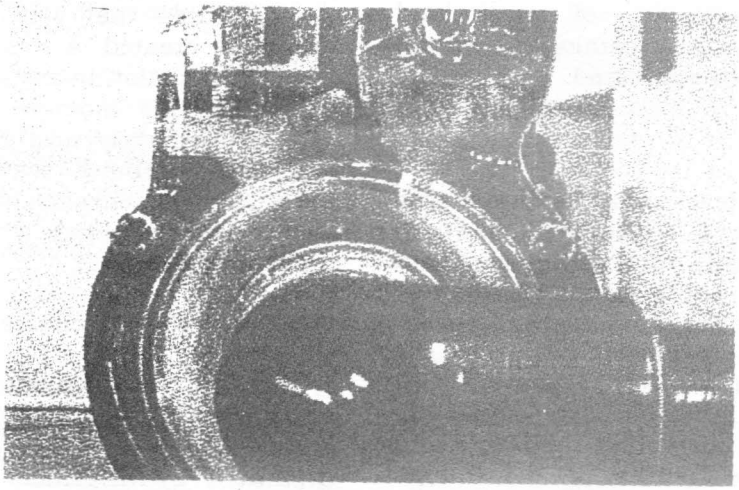

Photo. 5. Milky water color as a result of air bubbles.

the right side of this curve. The dangerous zone of pump operations is that on the right side of the critical trend. Also it is obviously clear from the results that the critical submergence increases with increasing the rotational speed. Increasing the rotational speed means more discharge and higher suction velocity, thus lower suction pressure. That means a higher discharge required large submergence in order to avoid the air entraining vortices. No vortices were observed at any speed with the submergence above 35 cm. The trend presented in Fig. 3 agreed with Elshorbagy and warda [7].

As mentioned before the data recorded in Fig. 3 was based on the visual observation of vortices. But that doesn't mean that, at these particular submergence, the vortex behavior will not be changed. In reality the vortex behavior changes significantly. It appears and disappears as a function of time.

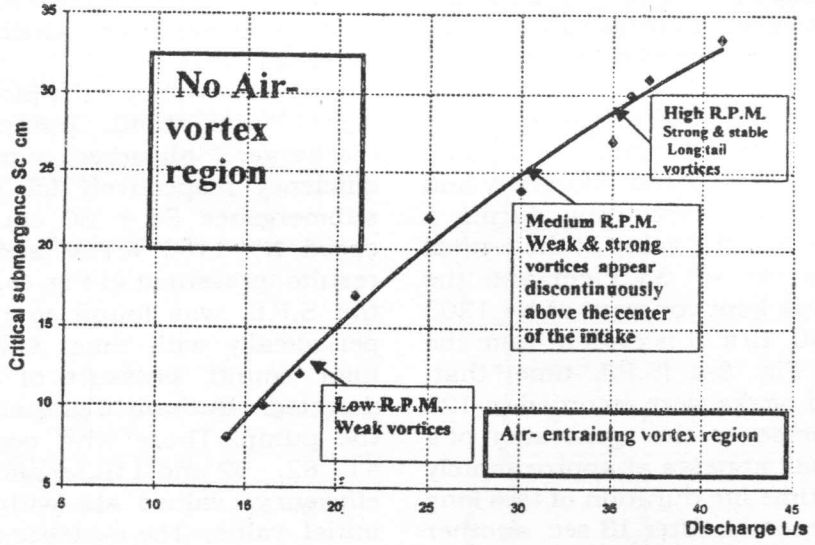

Fig. 3. Variation of critical submergence with pump speed.

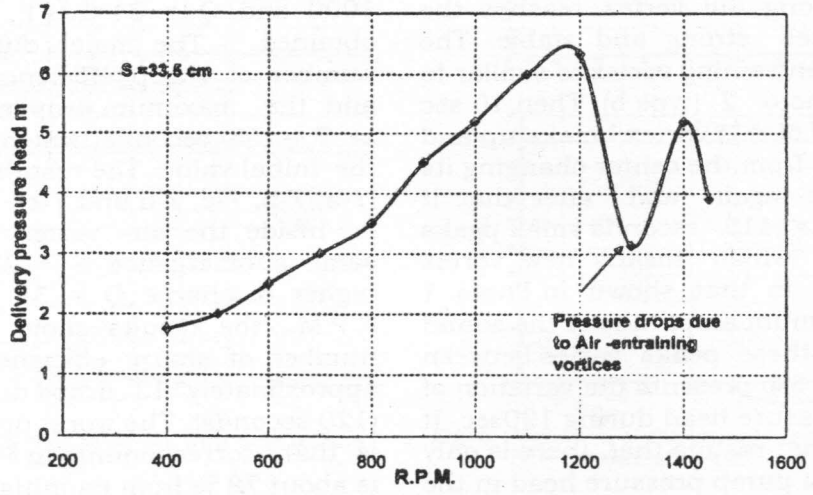

Fig. 4. Variation of the delivery pressure head with pump speed.

The behavior of air entraining vortex and its effect on the pump performance are investigated for at least 10 different values of critical submergence. As an example, we will present only four different values of critical submergence and will spot the change in all parameters. These values are Sc = 33.5 cm, 30cm, 27cm at 1000 R.P.M. and 27cm at 1200 R.P.M.

The results of the delivery pressure head when the rotational speed was increased by a step of 100 R.P.M are plotted in Fig. 4. It is clear that, The delivery pressure increases parabolically with pump speed up to 1100 R.P.M., and then drops randomly as speed increases above 1200 R.P.M., this is due to the effect of strong air entraining vortices.

Figure 5 shows the plot of the recorded values for the microphone signal, total pump pressure head, discharge, and efficiency and absorbed motor power respectively during a test period of 120 sec. The value of the critical submergence was Sc = 33.5 cm and the rotational speed was kept constant at N= 1203 R.P.M and Q = 40 L/s. It is evident from the results shown in Fig. 5-a (S.P.L.-time) that, four distinguished peaks were recorded in 120 sec. Each peak presents the generation of a vortex. The first peak appears at approximately T = 46 sec. the time life duration of this long tail vortex is 7 seconds. After 13 sec, another noisy vortex was born This long tail vortex as shown in Photo. 3 (type c), moves toward the center of the pump intake.

As soon as the long tail vortex reaches the center, it becomes strong and stable. The shape of this air-entraining vortex is similar to that shown in Photo. 2 (type b). Then 10 sec later, the stability of this vortex breaks up and then moves away from the center changing its shape to type c again and after that it disappears. At T = 115 seconds small peaks start to appear, which means new vortex generation similar to that shown in Photo. 1 (type a). The maximum amplitude of the sound pressure level of these peaks varies between 94- 97 dB. Fig 5-b presents the variation of the total pump pressure head during 120sec. It is evident from the results that, there is only one sharp drops in pump pressure head in the region where type b occurred. At T= 75 seconds, the pressure drops by 3 m which is a bit more than 50 % from its initial value and no evidence for another pressure drop due to vortices (type c and a) was recorded. Referring to Fig. 5-c, it is shown that at T= 75 seconds, the discharge was also affected and it was reduced by 7 L/s which is about 18 % from its initial value. From Fig. 5-d, one can see that there is a power drop by 500 watts which represents 12.5 % of its initial value and occurs only at T= 75 sec.

The variation of the overall efficiency of the pumping system is shown in Fig. 5-e. It is clear that, at the same region where the stable air-entraining vortex appeared there is a sharp drop in the efficiency, which is about 40% from its initial value.

Figure 6 shows the plot of the microphone signal, the total pump pressure head, discharge, absorbed motor power and efficiency respectively for the case of critical submergence Sc = 30 cm and the rotational speed N= 1150 R.P.M and Q = 39 L/s. The results presented in Fig. 6-a demonstrate that, the S.P.L. was found to rise and fall almost periodically with time. Almost 12 peaks with high sound pressure of about 96 dB were detected. But only 6 of them could affect badly the pump. Those who occurred at T= 26, 30, 41, 82, 92 and 110 seconds. The drops in the efficiency values are within 53 % from the initial value. The evidence is shown in figs. (6-b, 6-c, 6-d, and 6-e).

With further reduction in the submergence and discharge or R.P.M.(S c = 27 and R.P.M. = 1000 and Q = 34 L/s) , similar results were obtained . The major difference is that the number of sharp efficiency drops becomes 3. and the maximum drop in efficiency occurred at T = 55 seconds which is about 55 % from the initial value. The results are shown in Figs. (7-a, 7-b, 7-c, 7-d and 7-e).

Inside the air- vortex region and for the same submergence S = 27 cm but with a bit higher discharge Q = 38 L/s, and N= 1200 R.P.M., the results show an increase in the number of sharp efficiency drops; it becomes approximately 13 drops during the test period (120 seconds). The worst drops in the efficiency is that, corresponding to T= 60 seconds which is about 78 % from its initial

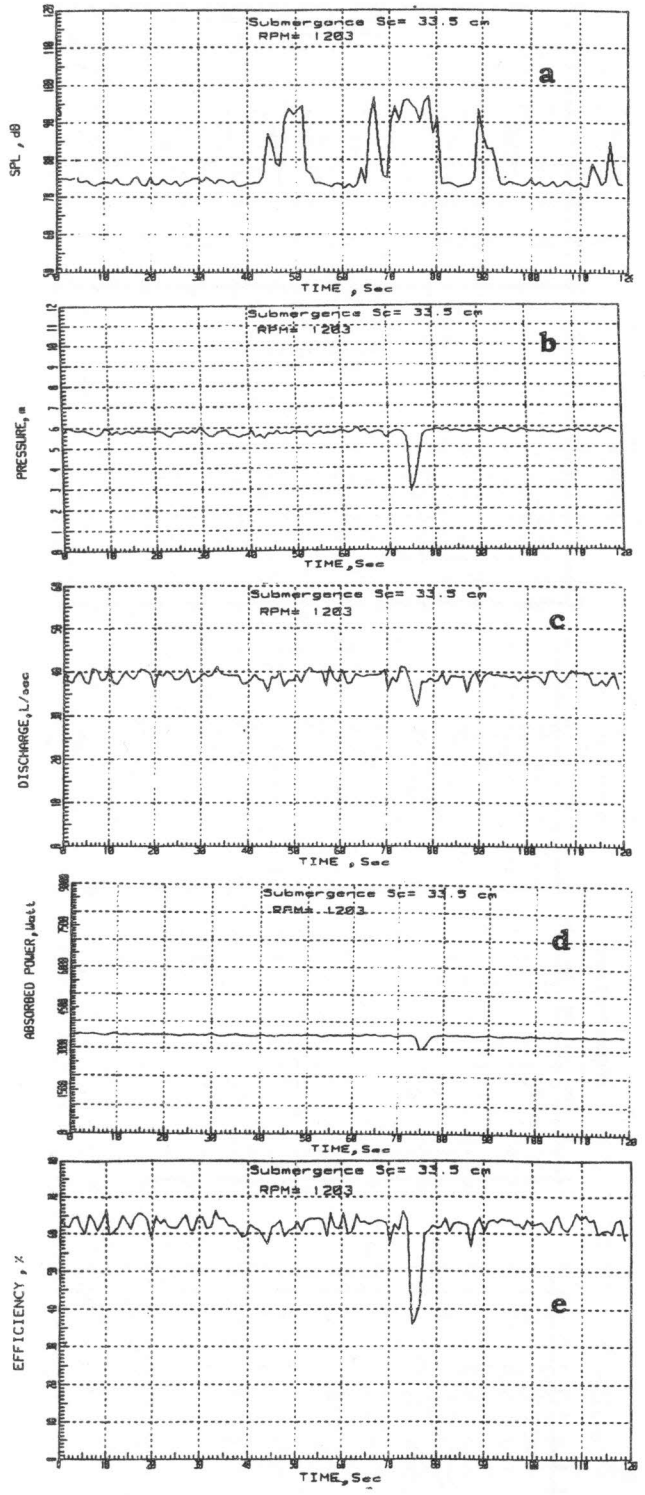

Fig. 5. Variation of the pump's pressure with time at Sc = 33.5 cm, R.P.M= 1203.

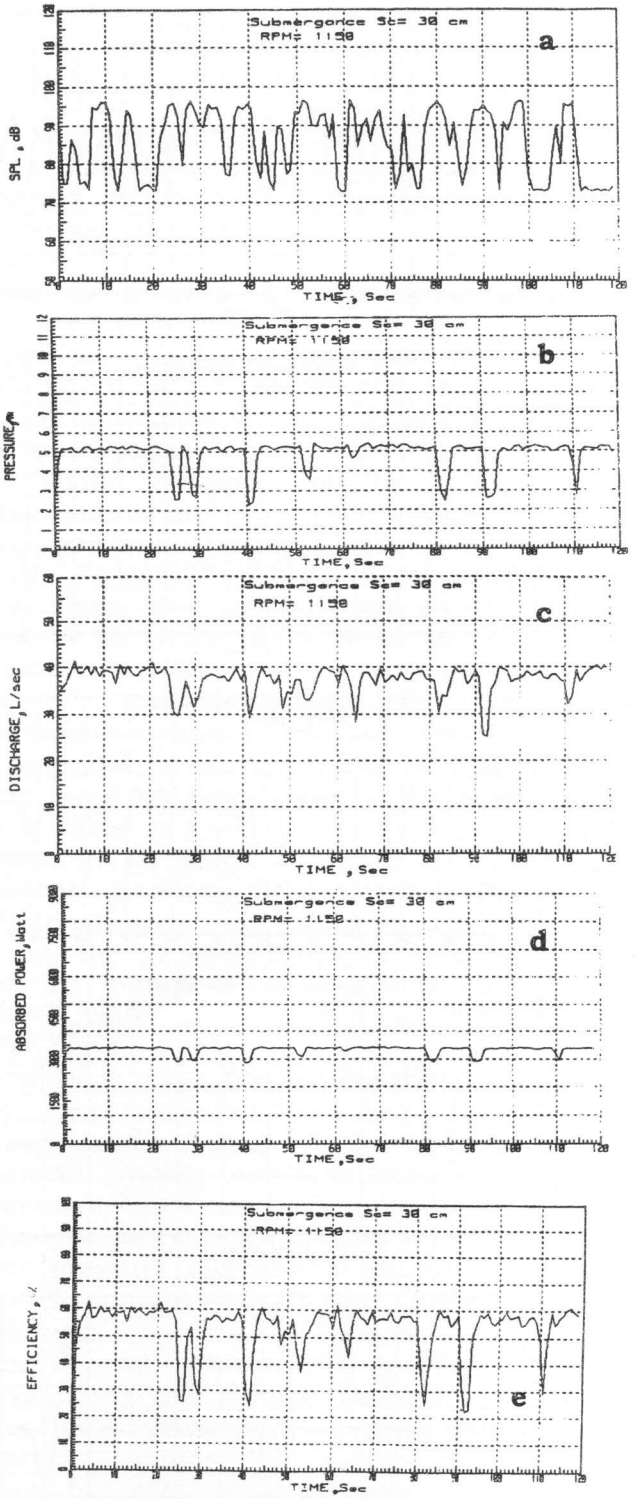

Fig. 6. Variation of the pump's performance with time at Sc = cm, R.P.M= 1150.

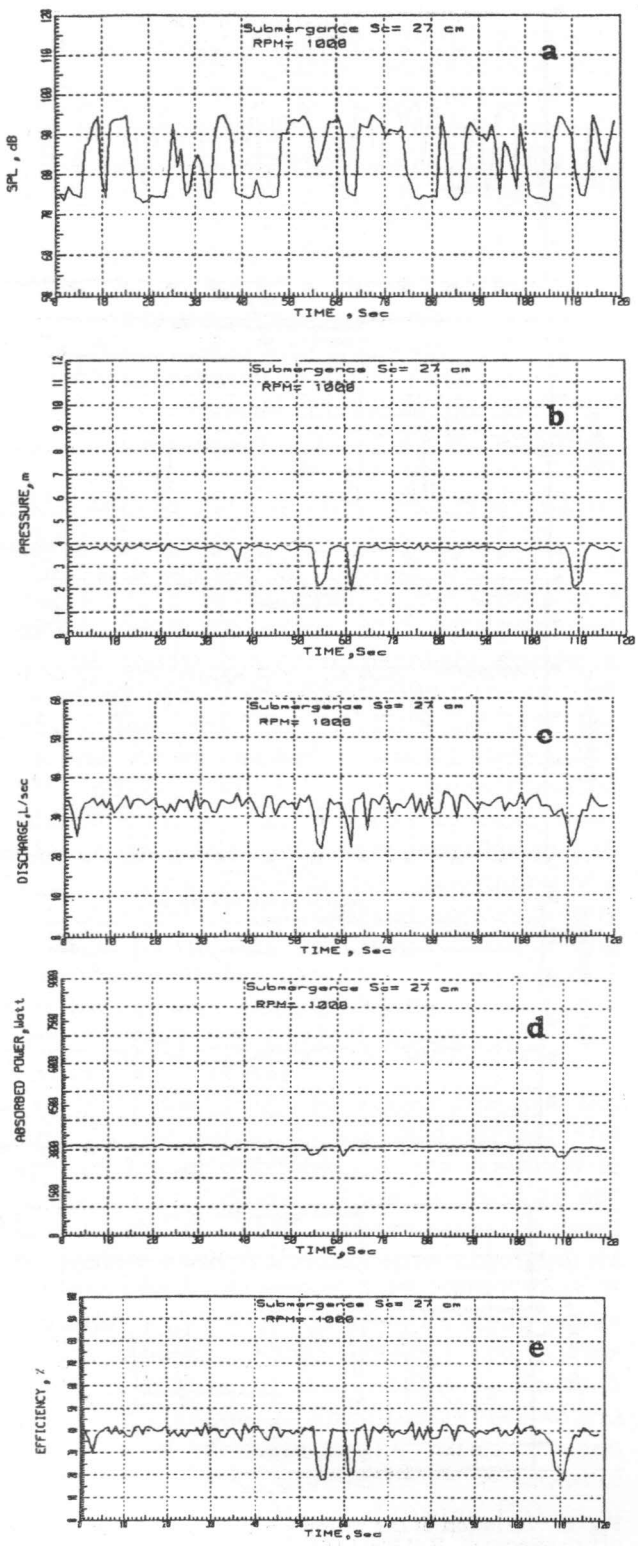

Fig. 7. Variation of the pump's performance with time at Sc = cm, R.P.M = 1000

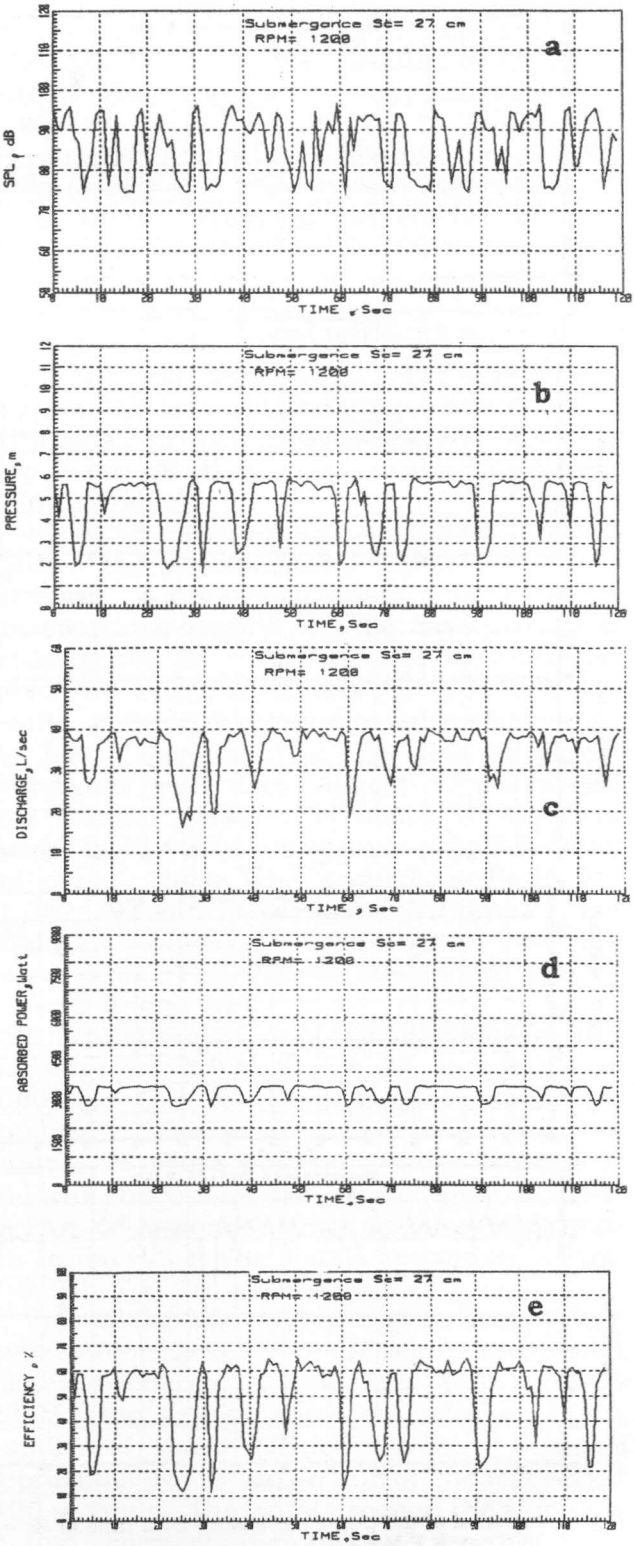

Fig. 8. Variation of the pump's performance with time at Sc=27 cm, R.P.M = 1200 (Inside the air-entraining region)

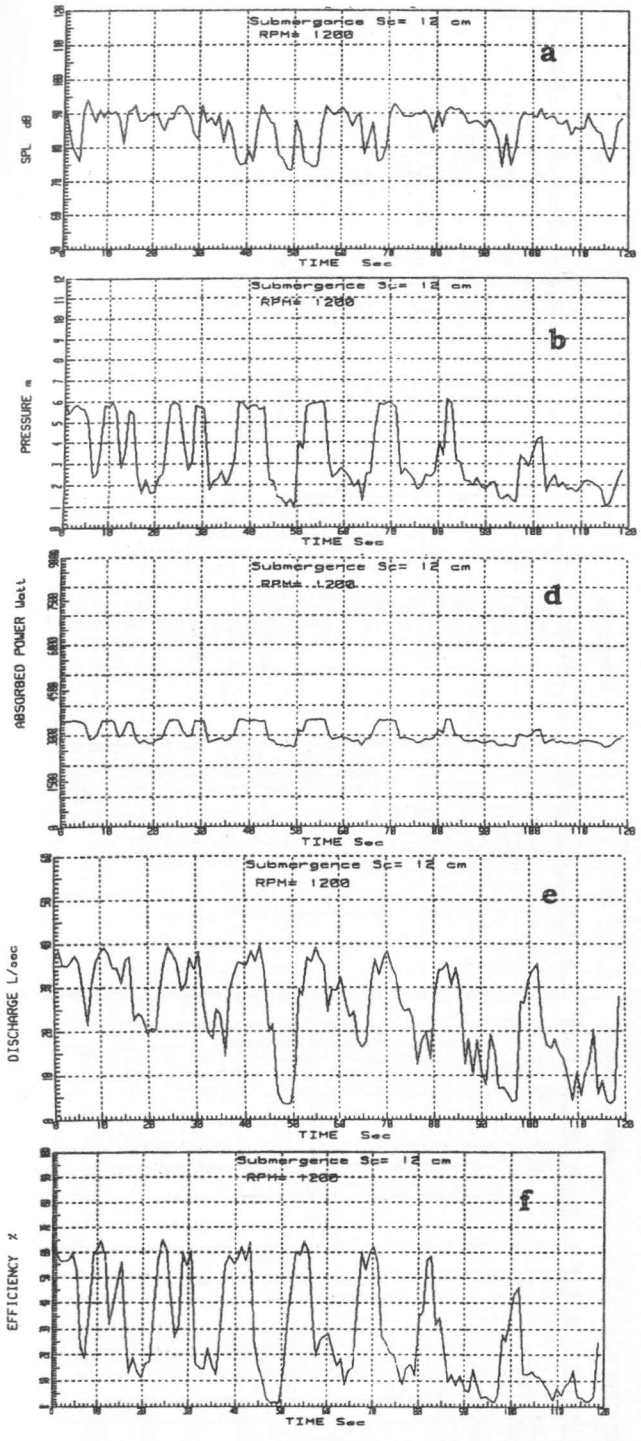

Fig. 9. Variation of the pump's performance with time at Sc=12 cm, R.P.M. =1200 (Inside the air-entraining region).

value. The results are shown in Figs (8-a, 8-b, 8-c, 8-d and 8-e).

At the submergence S = 12 cm and speed of 1200 R.P.M. it is clear from the results plotted in Figs. (9-a, 9-b, 9-c, 9-d and 9-e) that, at low submergence, all the above parameters are fluctuated. These fluctuations are large enough to warrant special protection measurements. The absorbed input power fluctuated 10 times during the specified test period, (120 seconds) whereas the efficiency drops to nearly zero value. That is due to the existence of (type d) vortices (Photo. 4). This kind of vortices absorbs a large quantity of air resulting in a significant drop in pump pressure head, and discharge with a slight drop in input power, this consequently accompanied by a severe drop in pump overall efficiency. The variation of sound pressure can be related to the discontinuation in vortex formation. Operating the pump in this region may result in serious and undesirable effects, which may lead to damaging the pump components. Fig. 10. shows the plots of the above parameters with respect to time. In this test, the frequency inverter variable speed drive was set to automatic operation so that the speed of the pump can be automatically adjusted to meet the head and flow demands. The submergence was taken as S = 26 cm whereas the rotational speed is an unknown value. The results are shown in Figs. (10-a to 10-f). The results demonstrated that, as far as a vortex (type b) form, the pressure drops, the rotational speed of the pump is automatically increased to compensate the drop in pressure. Comparing the results presented in Figs. (10-b and 10-c) with each other, one can see that the sequence of the pressure head and that of the rotational speed is the same. That means the automatic control system tends to keep the pressure constant but it has to increase the speed when the pressure drops and reduce the speed when the pressure increased resulting in the R.P.M. fluctuation shown in the interval of time between T = 7 and T =16 seconds. Similarly for the interval between T=57 and T= 71 seconds. Examining the plots of the S.P.L. against time Fig.(10-a) revealed that, there existed some vortices characterized by high sound pressure level but with negligible effect on either the pressure or the discharge level. This can be also seen in the R.P.M. plots in the interval between T=16 and, T= 57 seconds and T =71 up to 120 seconds. The effect of air-

entraining vortices on the discharge, efficiency and power is self-exploring in Figs. (10-d to 10-f).

Figure 11 indicated that for low submergence, Sc = 16 cm, the rapid changes in the rotational speed of the pump affect badly almost all pump parameters. This effect is mainly due to the fact that when the delivery pressure drops due to air entraining vortices, the rotational speed is increased creating a more vacuum pressure at the pump suction side. The vortices will hold at the pump intake for longer period of time introducing more air inside the pump. That means lower delivery pressure and again the rotational speed will increase or decreased to compensate the pressure fluctuations. It is worth noticing from Fig. (11-a) that the time duration of the first air-entraining vortex (type d) was about 55 seconds, during which the pressure fluctuated up and down almost 3 times. The fluctuation of the pressure 3 times in 55 seconds means that, the air was rejected from the pump 3 times during the 55 seconds. When air has been rejected from the pump the delivery pressure jump up and when air entering the pump the pressure drops and so on. The second generation of air entraining vortices is in the interval between T =70 and 120 seconds. The time lag between the break down of the first vortex and the generation of the second one is about 15 seconds. That can be detected from the plot of the S.P.L. Fig. (11-a) about 75 dB. It can also be detected from the pressure plot Fig. (11-b) in the region where the pressure head was maintained constant at 4.8 m. The significant fluctuations in the discharge, input power and efficiency are shown in Figs. (11-c, 11-d, 11-e and 11-f) demonstrate that the application of automatic control system with variable speed frequency inverter in the region where air-entraining vortices appears, may lead to a serious pump failure or even damages the pump components.

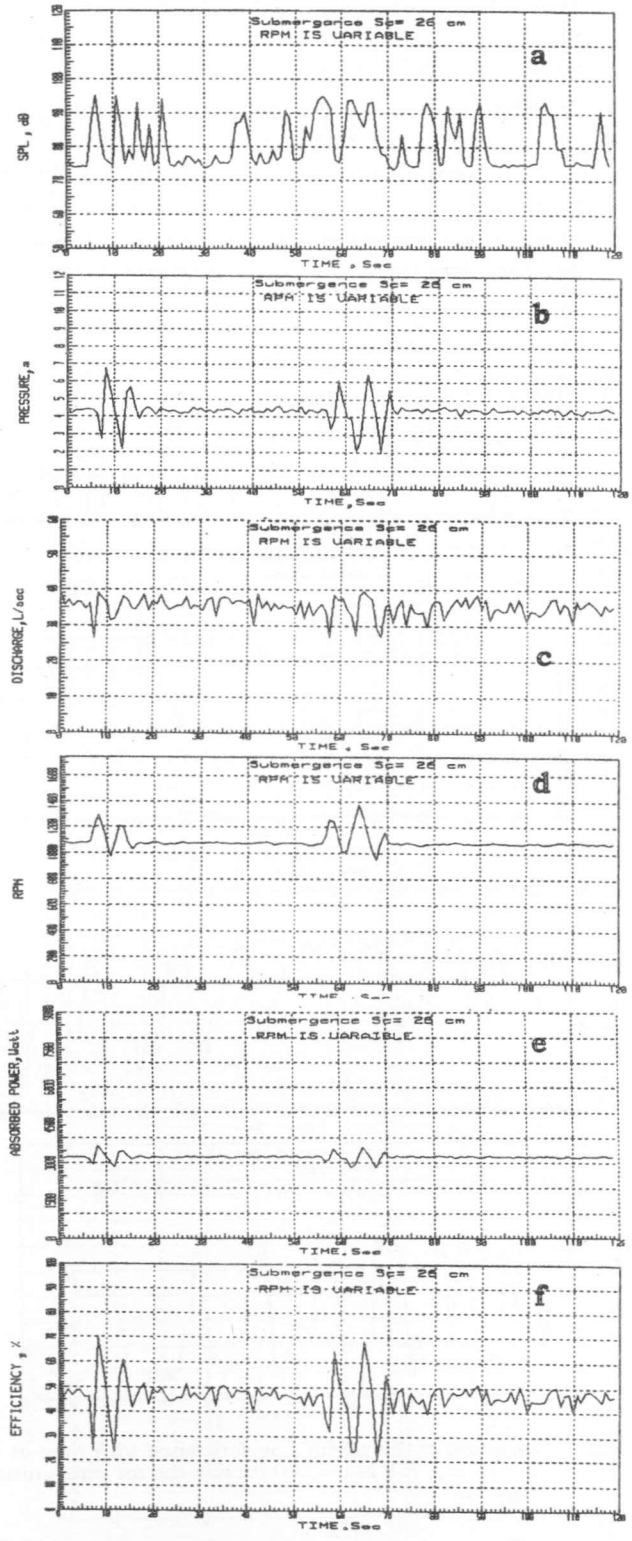

Fig. 10. Variation of the pump's performance with time at Sc =26 cm, R.P.M. is variable

6. Conclusions

The following conclusions can be deduced from the obtained results:

The technique of using the microphone signals (S.P.L.) in conjunction with the

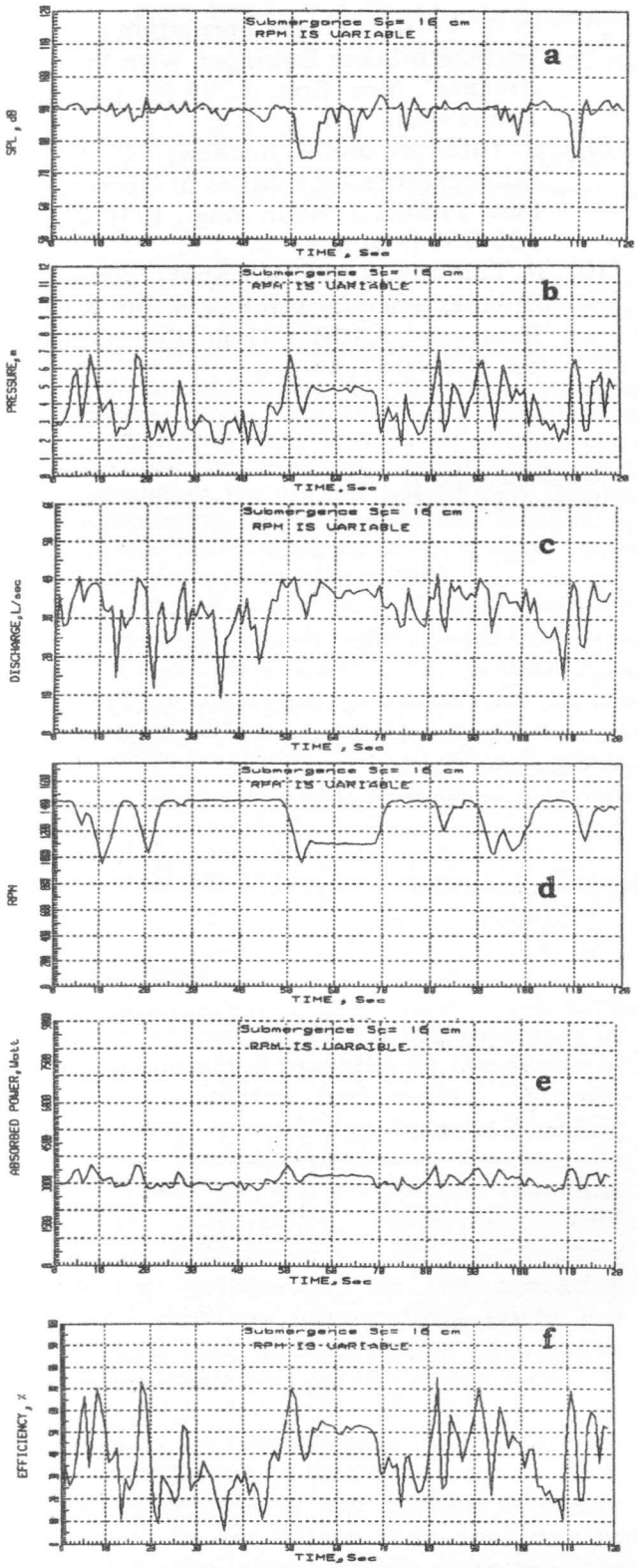

Fig. 11. Variation of the pump's performance with time at Sc = 16 cm, R.P.M. is variable.

pressure transducer (pressure head) was found to be useful in understanding the vortex behaviors.

The air-entraining vortices under severe conditions have a harmful effect on pump performance through decreasing pump pressure head, discharge and efficiency. The quick response of the automatic control system for pump speed variation results in rapid pressure fluctuations and sharp drops in efficiency. This makes the application of automatic control system in the air- vortex region is undesirable. It can bring unstable operation to pump and after certain period of time it may damage the pump components.

Acknowledgements

This study has been financed by "National Council for Scientific Research", Beirut-Lebanon. This support is greatly appreciated.

Notation

Cos ϕ	is the power factor.
D	is the internal diameter of the suction pipe.
h	is the total pump head.
I	is the current (Ampere).
N	is the rotational speed (R.P.M).
P	is absorbed power.
Q	is the average discharge of the pump (L/s).
S	is the submergence (Vertical distance between water surface and intake tip).
Sc	is the critical submergence (Critical value of S).
S.P.L.	is the sound pressure level detected by a 1/2 microphone.
T	is the time in seconds.
V	is the voltage.
γ	is the water specific weight, (kN/m^3).

References

[1] D.F. Denny "An Experimental Study of air-Entraining Vortices in Pump Sumps", Proc. of the Institute of Mechanical. Engineers, London, England, 107(2), pp.106-116 (1956).

[2] D.F Denny and G.A. Young "The Prevention of Vortices and Swirl at

Intakes", Proc. Of IAHR 7 th Congress, Lisbon, pp. C1-8 (1957).
[3] H. O. Anwar, "Flow in a Free Vortex", Water Power (Apr.), pp. 153-161 (1965).
[4] H.O. Anwar, "Prevention of Vortices at Intakes", Water Power (Oct.), pp. 393-401 (1968).
[5] A.J. Odgaard, "Free Surface Air Core Vortex", J. of Hydr. Eng. Div., ASCE, 112 (7), pp. 610-620 (1986).
[6] K. J. Jain R.K. Raju and J.R. Garde (Oct) "Vortex Formation at Vertical Pipe Intakes", J. of Hydr. Eng. Div., ASCE, HY10, pp. 1429-1445 (1978).
[7] K. A. Elshorbagy and H.A. Warda "An Investigation of Cavitation Noises at the Inverted Intake of a liquid Basin" Alex. Eng. J., 29 (4), pp. 259-268 (1990).
[8] H. A. Warda, "Vortex Formation at Vertical Intakes Equipped With Vortex Breaker", Alex. Eng. J., 29 (4), pp. 189-195 (1990).
[9] N. Yuldirim, and F. Kocabas, "Critical Submergence for Intakes in Open Channel Flow", ASCE J. Hydr. Eng., 121(12), pp. 900-905 (1995).
[10] N. Yuldirim, and F. Kocabas, " Critical Submergence for Intakes in Still Water Reservoir", ASCE J. Hydr. Eng., 124 (1), pp. 103-104 (1998).

Received December 25. 1999
Accepted January 6, 2000